Environmental Science & Technology

ARTICLE

pubs.acs.org/est

Effects of Nano Zero-Valent Iron on Oxidation−Reduction Potential

Zhenqing Shi, James T. Nurmi, and Paul G. Tratnyek*

Division of Environmental and Biomolecular Systems, Oregon Health & Science University, 20000 NW Walker Road, Portland, Oregon 97006, United States

Supporting Information

ABSTRACT: Oxidation−reduction potential (ORP) measurements have been widely used to assess the results of injection of nano zerovalent iron (nZVI) for groundwater remediation, but the significance of these measurements has never been established. Using rotating disk electrodes (RDE) in suspensions of nZVI, we found the electrode response to be highly complex but also a very sensitive probe for a range of fundamentally significant processes. The time dependence of the electrode response reflects both a primary effect (attachment of nZVI onto the electrode surface) and several secondary effects (esp., oxidation of iron and variations in dissolved H_2 concentration). At nZVI concentrations above ~200 mg/L, attachment of nZVI to the electrode is sufficient to give it the electrochemical characteristics of an Fe^0 electrode, making the electrode relatively insensitive to changes in solution chemistry. Lower nZVI concentrations give a proportional response in ORP, but much of this effect is mediated by the secondary effects noted above. Coating the nZVI with natural organic matter (NOM), or the organic polymers used to make stabile suspensions of nZVI, moderates its effect on ORP measurments. Our results provide the basis for interpretating ORP measurements used to characterize the results of injecting nZVI into groundwater.

INTRODUCTION

The injection of nanosized zerovalent iron (nZVI) for remediation of contaminated groundwater is one of the most prominent examples of the application of nanotechnology for environmental improvement.[1−3] Numerous laboratory studies of the physicochemical aspects of this technology have been reported, including methods of nZVI synthesis, modification, and handling (e.g., refs 4−7); the structure and composition of nZVI and its aggregates (e.g., refs 8−10); the reactions of nZVI with contaminants and natural solutes (e.g., refs 11−13); and the transport and fate of nZVI in porous media (e.g., refs 14−17). At the same time, there have been many applications of this technology in the field, including a few study sites that were subjected to fairly detailed characterization of the results.[18−21] Predictably, however, these field studies are characterized in less detail than the laboratory studies, and this gap has made it difficult to fully reconcile several key differences between the laboratory and field behavior of nZVI.

One of the most fundamental differences of this type concerns the methods used to detect nZVI during and after injection. There are few sensitive and specific methods for *direct* detection of any type of anthropogenic nanoparticles in environmental media,[22] and there is no proven protocol for direct detection of nZVI in the field. Instead, the field studies reported so far (as well as many laboratory column studies) have relied on monitoring methods that are *indirect* in that their response is not necessarily to the nZVI *per se* but rather is mediated by products of reaction between Fe^0 and the medium. These reactions—which have been summarized many times (e.g., ref 23)—consume dissolved O_2 and reducible contaminants (sometimes generating diagnostic products), generate Fe^{II}/Fe^{III} species and H_2, increase the pH, and lower the Eh. Anticipating these effects, the corresponding groundwater properties are usually measured at sites where nZVI is injected into the subsurface, and when the expected trends are observed, they are interpreted as evidence that the emplacement was successful.[19,20]

However, further consideration of the basis for this interpretation suggests that complex relationships are to be expected between the observed changes in these groundwater properties (Eh, pH, etc.) and the transport of nZVI impacted fluids. For example, all of the observed changes are the result of reactions between nZVI and the medium, so as the nZVI is consumed and/or passivated by these reactions it should have diminishing effects on the solution chemistry, resulting in decreased sensitivity of these methods to the residual nanoparticles. Complications such as this can be, at least partially, obviated by interpreting the corrosion-linked changes in measured solution properties as evidence of nZVI *reactivity* rather than transport. Adopting this shift in emphasis, the open-circuit potential measured at an inert electrode (commonly and herein referred to as ORP, for oxidation−reduction potential) acquires special significance because of its unique relationship to the whole range of redox-related processes in environmental systems.

Although a great deal has been written about the measurement and interpretation of ORP in natural media (e.g., refs 24−28), and ORP has frequently been used to characterize field sites where nZVI was injected,[18,20] there is considerable uncertainty about the meaning of ORP measurements made in the presence of nZVI. The key considerations are summarized in Figure 1 and discussed below. The processes shown in Figure 1 combine to determine the measured ORP, which is a mixed potential (E_{mix}) composed of the weighted sum of Nernstian terms (in square

Received: September 18, 2010
Accepted: December 14, 2010
Revised: December 9, 2010
Published: January 4, 2011

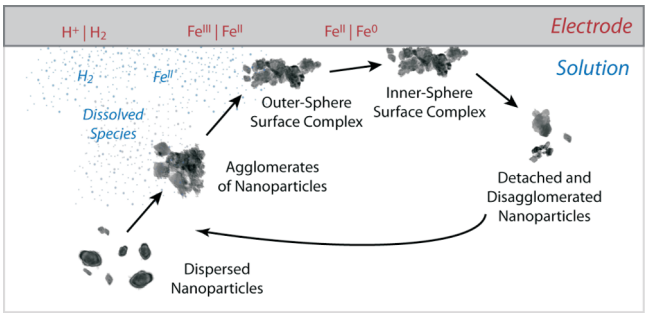

Figure 1. Anticipated interactions between an electrode (red), aqueous solution (blue), and nanoparticles of zerovalent iron (black).

brackets in eq 1) for each of the redox couples that are present at the electrode surface[29]

$$E_{mix} = \sum_{i=1}^{m} \frac{|i_i^0|}{\sum |i_i^0|}\left[E_i^0 - \frac{RT}{n_i F}\frac{\{\mathrm{Red}_i\}}{\{Ox_i\}\{H^+\}^a}\right] \quad (1)$$

For each half-reaction between a reduced species (Red_i) and oxidized species (Ox_i), eq 1 includes the corresponding values of exchange current density (i^0), and the stoichiometric coefficients for electrons (n) and protons (a). In the typical application of eq 1 to interpretation of ORP measurements, Red_i and Ox_i are dissolved species in redox couples that interact with the electrode only through electron transfer. Redox couples that meet these conditions and are likely to be important in solutions containing nZVI include H_2/H^+ and various dissolved phase complexes of Fe^{II} and Fe^{III}. However, redox couples involving solid phase species (FeOOH, Fe_3O_4, Fe^0, etc.) also may be significant, but accommodating them in eq 1 raises numerous issues related to the effects of particle size, structure, and composition on electrode response.

The general problem of interpreting potentiometric data obtained in colloidal suspensions has been subjected to theoretical and experimental investigations,[30] which have identified two distinct types of effects. One type of effect arises at the liquid junction of the reference electrode due to interactions of the internal electrolyte with the external suspension, and this usually can be minimized by judicious experimental design.[31,32] The other type of effect stems from interactions between the double layers of the indicator electrode and the suspended particles in the sample.[33] This can be a major complication for some applications (e.g., pH measurement in turbid environmental waters[32]) but could be part of the basis for the sensitivity of ORP measurements to nZVI (the focus of this study). A suspension effect of the latter type requires particles that are large enough to have their own well-defined Gouy−Chapman type double layers,[30,33] which is consistent with the primary particle size of most types of nZVI that are currently in use (40−60 nm[9]). However, suspensions of nZVI also contain variable quantities of large aggregates (which presumably have no direct effect on the indicator electrode response) and small nanoparticle precursors (which can give effectively Nernstian electrode response even though these very small particles are not thought to contribute directly to the exchange current[34,35]).

In addition to the above considerations for potentiometric measurements made in the presence of suspended particles, there could also be effects on the redox properties *of* the particles—if the particles are sufficiently small (<2−4 nm[36,37])—that could propagate to changes in measured ORP. Specifically, it has been shown theoretically that the redox potential of nanoparticles should be considerably more cathodic than the corresponding bulk material for both metals[38] and semiconductors,[39] which together should determine the electronic properties on nZVI.[40] In fact, a cathodic shift in open-circuit potential has been observed using electrodes made from nZVI,[9] although it is not yet clear that the latter observation is a direct manifestation of the theoretically predicted behavior. Regardless of its source, the possibility that this effect influences measurement of ORP on suspensions of nZVI is a further complication that needs to be understood before such measurements can be a reliable indicator of the results of nZVI injection for subsurface remediation.

Given the number and scope of the uncertainties in how ORP measurements respond in suspensions of nZVI, it is unlikely that this measurement—as commonly applied—will ever provide unambiguous evidence of nZVI transport in environmental media. However, the considerations summarized above also suggest that more innovative applications (or interpretations) of ORP measurements could prove to be a powerful probe of a variety of questions regarding the environmental fate and effects of nZVI. To investigate this, we compare amperometric measurements obtained using powder-disk electrodes (PDEs) made with nZVI and potentiometric measurements with rotating-disk electrodes (RDEs) made of platinum (Pt) or glassy carbon (GC) and immersed in suspensions of nZVI of various types under a range of solution conditions. The results suggest that ORP measurements in the presence of nZVI are complex—but qualitatively explicable—mixtures of potentials that reflect the unique combination of redox and related processes that characterize these systems.

EXPERIMENTAL SECTION

Reagents. All solutions were made by dissolving high purity chemicals in Ar-sparged (deoxygenated) deionized water (DO/DI). The background electrolyte used in most experiments was 3.33 mM $NaHCO_3$ (pH 8.4−8.6). For comparison with results from previous work, 0.19 M borate buffer (pH 8.4) was used in a few experiments. Solutions containing 10−200 mg/L natural organic matter (NOM) in 3.33 mM $NaHCO_3$ were made by diluting a stock solution containing 200 mg/L of potassium humate solution (Leonardite Products LLC; Williston, ND).

Nano Zero-Valent Iron. The nZVI used in this study included RNIP-10DP and RNIP-M2 obtained from Toda America Inc. (Schaumburg, IL). RNIP-10DP is a solid powder that was protected from moisture during storage, whereas RNIP-M2 is provided as an aqueous slurry. Storage and all exposed handling of either material were done in an anoxic glovebox (5% H_2 in N_2). Stock suspensions containing 18 g/L nZVI were made by dispersing RNIP-10DP dry powder or diluting RNIP-M2 slurry in the background electrolyte. After first wetting the RNIP-10DP, these stock solutions were allowed 2 d of "preexposure" time to get past the initial period of rapid aging of the particles.[12] Immediately prior to use, the nZVI stock solutions were sonicated (Bronsonic 3210, Danbury, CT) for 30 min to disperse the particle aggregates. Various nZVI concentrations were obtained by diluting the nZVI stock solution with additional background electrolyte.

Electrochemical Experiments. Working electrodes made from platinum (Pt, 3.0 and 5.0 mm dia.) and glassy carbon (GC, 5.0 mm dia.) disks were obtained from Pine Instruments (Grove City, PA). The PDEs of nZVI were of the same design

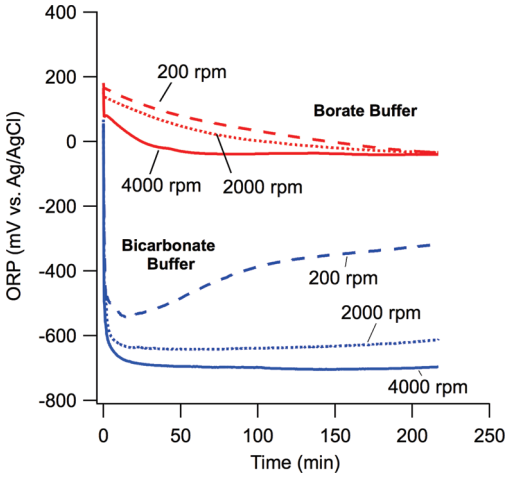

Figure 2. Temporal evolution of ORP obtained with a 3 mm Pt RDE in suspensions of nZVI (200 mg/L RNIP-10DP). Upper (red) set for 190 mM borate at pH 8.4; lower (blue) set for 3.33 mM bicarbonate at pH 8.4. RPM speeds are labeled in the figure.

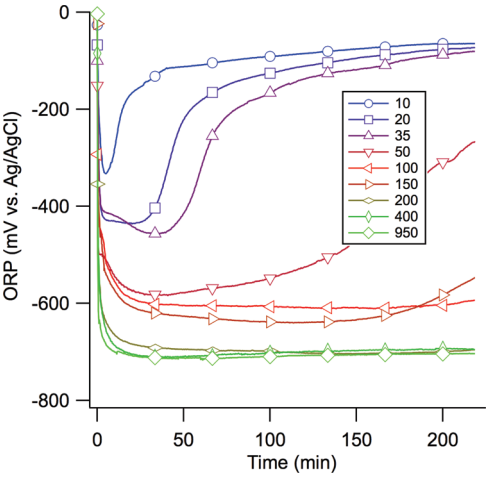

Figure 3. Temporal evolution of ORP vs concentration of nZVI (mg/L RNIP-10DP given in the legend). Conditions: 3 mm Pt RDE at 4000 rpm in 3.33 mM bicarbonate at pH 8.4. Markers shown every 200 data points.

that we have described and validated previously.[9,12,41,42] Reference electrodes (Ag/AgCl) filled with the AgCl saturated 3 M NaCl solution were obtained from Bioanalytical Systems, Inc. (West Lafayette, IN). Additional details on the fabrication and validation of the electrodes used in this study are given as Supporting Information.

RDE experiments were conducted by rotating Pt or GC electrodes and continuously recording ORP—as the open-circuit potential vs the Ag/AgCl reference electrode—using a potentiostat. Because of the high degree of control afforded by the RDE-based experimental design, we used this system to study the effects of mixing, nZVI concentration, particle aging and aggregation, and organic coatings. Detailed information on the RDE reactors, rotating speeds, and operating conditions can be found in the Supporting Information.

RESULTS AND DISCUSSION

Effects of Mixing. In addition to the effect of nZVI aging—which we controlled with the preexposure period justified in Section 1 of the Supporting Information—key experimental design considerations for ORP measurements made on suspended nZVI are managing the effects of particle settling, aggregation (intraparticle), and attachment (esp. to the electrode surface). Controlling these processes was greatly facilitated by using an RDE, and varying the rotation rate of the RDE allowed us to systematically investigate the effects of these processes on ORP measurements. The high quality of the resulting data is demonstrated in Figure 2, which shows the effect of rotation speed (RPM) on ORP vs time in two buffer systems, borate and bicarbonate. In all cases, the data show smooth transitions to relatively stable values, and these transitions occurred more rapidly at higher RPM. The more negative values of ORP obtained at higher RPM could be due to (*i*) greater contact between the nZVI particles and the electrode surface due to the thinner boundary layer at the electrode and/or (*ii*) higher concentrations of nZVI in the general vicinity of the working electrode due to greater mixing of the bulk solution. Unlike the former (boundary layer) effect, the latter (settling) effect should be strongly dependent on operational aspects of the experimental design, as discussed in the Supporting Information (Section 2).

Effects of nZVI Concentration. Central to all aspects of this study is the relationship between ORP and the concentration of suspended nZVI ([nZVI]). For concentrations of nZVI ranging from 10 to 950 mg/L RNIP-10DP, measurements of ORP vs time were made using a 3 mm Pt RDE (Figure 3), 5 mm Pt RDE (Supporting Information, Figure S1-B), and 5 mm GC RDE (Supporting Information, Figure S1-C). A similar range of nZVI concentrations (5−800 mg/L) was tested with RNIP-M2 using a 5 mm GC RDE (Figure S1-D). In all cases, upon diluting the nZVI stock solution into the measurement solution, the ORP decreased quickly (presumably due to a combination of rapid electrode polarization and solution equilibration effects) and then approached a minimum value (ORP_{min}) usually within ~50 min. At most concentrations of nZVI, the ORP stayed low (close to ORP_{min}); although a characteristic rebound was observed at low nZVI concentrations (e.g., at <50 mg/L in Figure 3), which is discussed later.

For each combination of nZVI and electrode type, the ORP_{min} decreased with increasing concentration of nZVI, but the relationship between these variables is highly nonlinear (Supporting Information, Figure S2), suggesting a complex response function that is unlikely to be usable as a calibration curve. When plotted as ORP_{min} vs log [nZVI], as shown in Figure 4, the data for low [nZVI] suggest an approximately linear relationship, which is consistent with a Nernstian dependence of ORP_{min} on [nZVI]. However, at [nZVI] greater than about 100 mg/L, ORP_{min} becomes relatively insensitive to [nZVI], and the data even suggest a plateau or limiting value of ORP (ORP_{lim}). At the end of these experiments, the electrode surface appeared to be covered with a film of nZVI derived particulate material, suggesting that the decreased sensitivity of ORP_{min} at high [nZVI] is due to increasingly complete coverage of the electrode surface. This effect is unsurprising given the strong tendency of nZVI to deposit onto all types of surfaces,[17] but the magnitude of the effect is notable because it suggests that the primary determinant of ORP response under conditions like those studied here (as well as those used in field applications of nZVI) will be the direct effect of nZVI attachment to the electrode.

This interpretation of the ORP_{min} vs [nZVI] data suggests that the trend (shown in Figures 4 and S2) may have the same form as

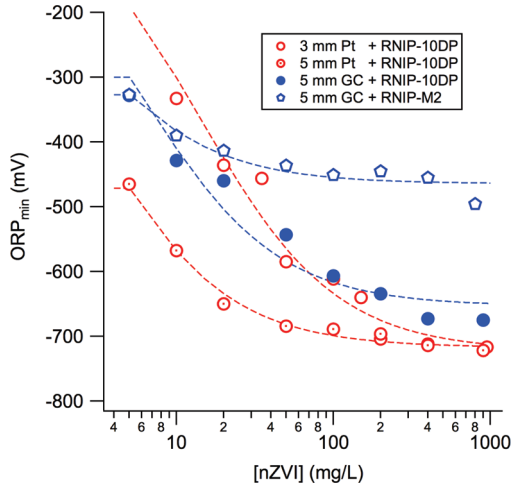

Figure 4. Minimum ORP (ORP_{min}) vs nZVI concentration, determined from data in Figure 3 and Supporting Information, Figure S1. The curves are from fitting the data to eq 2, and fitting coefficients are given in Table S1.

an adsorption isotherm. Using a Langmuir-type model to represent the apparent saturation effect seen in our data, we can write

$$ORP_{min} = \frac{ORP_{lim} K'_d [nZVI]}{1 + K'_d [nZVI]} \quad (2)$$

where ORP_{lim} (mV) and K_d' (L mg^{-1}) are analogous to the saturation and affinity constants in other applications of Langmuir-type models. In this case, ORP_{lim} is the response of an electrode that is completely covered with nZVI particulate material, and K_d' is mainly the tendency of nZVI to deposit onto the electrode surface. Using eq 2 to fit the data for ORP_{min} vs [nZVI] gives the coefficients summarized in Table S1 (Supporting Information) and the smooth curves shown in Figures 4 and S2.

Defined in this way, ORP_{lim} should depend mainly on the composition of the particles that form the film on the electrode, but may also be influenced by secondary factors such as the concentrations of dissolved H_2 and Fe^{II} (cf., Figure 1 and discussion below). For 3 mm and 5 mm Pt electrodes, the fitted values of ORP_{lim} are not significantly different, and the representative value (−0.72 V vs Ag/AgCl) is consistent with limiting potentials measured by chronopotentiometry with stationary powder disk electrodes (PDEs) made from the same material (−0.75 to −0.80 V[4,9]). Compared to the values of ORP_{lim} obtained with the Pt RDE, the GC RDE gave more positive values for RNIP-10DP (−0.65 V), presumably because i^0 for H_2/H^+ is small for GC compared with Pt.[43,44] An even more positive value of ORP_{lim} was obtained with the GC RDE for RNIP-M2 (−0.46 V), likely due to the redox-inactive organic polymer that is used to stabilize suspensions of this material. Further support for these interpretations of the OCP vs time data can be seen in complementary electrochemical data obtained by linear sweep voltammetry (LSV), which are given as Supporting Information (Section 4).

In so far as K_d' reflects the tendency of nZVI to deposit on the RDE, it could provide characterization that is complementary to other means of quantifying particle attachment (e.g., a_s in the filtration model of Yao et al.[45]). However, while the fitted values of K_d' appear to be statistically different (Table S1), the variation in these values is insignificant relative to the range of [nZVI] studied (recall that $K_d' = 1/[nZVI]$ at $ORP_{lim}/2$). The lack of differentiation among the fitted values of K_d' could be because the early stage of nZVI attachment is controlled by nonelectrochemical processes (like mass transport), but it could also arise because K_d' is sensitive to secondary effects on the electrode response.

Secondary and Tertiary Effects. In addition to the primary potential-determining effect of nZVI deposition onto the electrode, secondary and tertiary effects on ORP measurements are evident at low [nZVI]. Secondary effects are due to species that arise as products of reactions involving the nZVI that then go on to contribute directly to the ORP through eq 1. The two types of secondary effects that are mostly likely to be significant involve Fe^{II} species and H_2, both of which are discussed below. Tertiary effects are those that arise from sources other than the nZVI. One example is the effect of O_2 intrusion on the speciation of iron, which seems to be the main cause of the rebound seen in our ORP vs time data at low [nZVI] (e.g., Figure 3). This tertiary effect is discussed in the Supporting Information.

Because the primary and secondary effects on ORP in this system are interrelated, it is difficult to isolate them experimentally. For this reason—and because the secondary effects will vary greatly with the dissolved H_2 concentration, Fe^{II} speciation and concentrations, and pH—it is useful to evaluate the potential significance of Fe^{II} species and H_2 with thermodynamic calculations. These calculations are presented in Sections 5 and 7 of the Supporting Information.

Thermodynamic calculations for iron species under the conditions relevant to this study (details in Supporting Information, Section 5) show that the lowest expected equilibrium potentials (E) range from −0.8 V vs Ag/AgCl at pH 8.5 (due to Fe^0/$FeCO_3$) to −1.4 V at pH 9.5 (for Fe^0/Fe_3O_4) (Figure S4). Recognizing that iron speciation in nZVI suspensions is likely to be significantly controlled by kinetics, we must also consider possible metastable species like $Fe(OH)_2$.[46] However, the corresponding thermodynamic potential for $Fe^0/Fe(OH)_2$ is similar to the others involving Fe^0, and they are all similar to the E for H_2/H^+ discussed below. The lack of clear differentiation among the equilibrium potentials for each couple that might be contributing to the mixed potential measured by ORP makes their actual contributions ill-defined.

For the H_2/H^+ couple, the equilibrium potential as a function of H_2 concentration and pH is given in Figure S6 (Supporting Information). Approximate regions of environmental relevance are highlighted in the figure, and these show that the E from H_2/H^+ should be 200−300 mV lower in proximity to ZVI than in naturally anoxic ground waters (−0.4 to −0.6 vs −0.1 to −0.4 V vs SHE). The range of E for H_2/H^+ expected in the presence of ZVI agrees well with values of ORP measured in this study with Pt electrodes (e.g., $ORP_{lim} \approx -720$ mV vs Ag/AgCl, Table S1) and ORP obtained with Pt in solutions sparged with 5% H_2 but containing no nZVI (Supporting Information, Figure S7). These results, together with the fact that i^0 for H_2/H^+ on Pt is large,[43,44] suggest that H_2/H^+ could be contributing significantly to the ORP measured with Pt in the presence of ZVI.

To further investigate the role of H_2/H^+ in this system, we compared ORP measured with Pt to GC, which is comparatively insensitive to H_2/H^+ (i^0 for H_2/H^+ on GC is small[47]). In solutions sparged with 5% H_2 but not containing any iron, Pt and GC give ORPs that differ by ∼700 mV (Supporting Information, Figure S7), which is a much larger difference than is observed in suspensions of nZVI (e.g., the difference in ORP_{lim} for 5 mm electrodes in RNIP-10DP is only 64 mV, Table S1). This observation

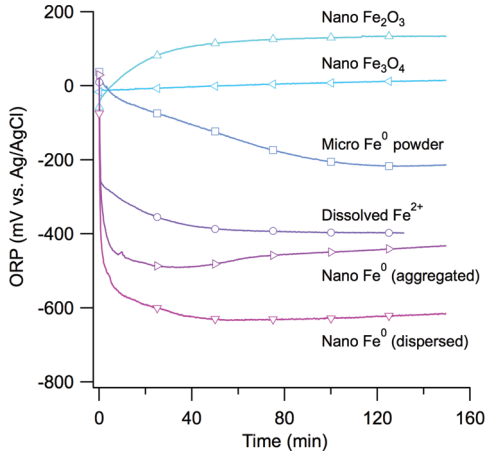

Figure 5. Temporal evolution of ORP (5 mm GC RDE at 900 rpm vs Ag/AgCl) of various Fe materials in 3.33 mM $NaHCO_3$ at pH 8.4. All particle concentrations are 200 mg/L. For dissolved Fe^{2+}, 0.1 mM Fe^{2+} was spiked into the $NaHCO_3$ solution, which is oversaturated according to the solubility of $FeCO_3$. Markers shown every 200 data points.

suggests that the ORP of nZVI suspensions is significantly influenced by redox couples that have more similar sensitivities to Pt and GC. Redox couples involving iron could be responsible for this effect, because it has been shown that Fe^{II}/Fe^{III} give similar responses on Pt and C electrodes.[48]

Effects of Particle Aging and Aggregation. The overall consistency of our interpretation of ORP measurements made on nZVI suspensions can be tested by comparison with measurements made on a range of related systems. For this, we measured ORP vs time profiles with a GC electrode to emphasize the role of Fe species over H_2 and with 200 mg/L concentrations of various particles to ensure stable ORPs (Figure 5). For reference, we show the data for 200 mg/L of dispersed (freshly sonicated) RNIP-10DP from Figure S1-C, which had an ORP_{min} of −650 mV vs Ag/AgCl. Without sonication, the nZVI is more aggregated, and this results in somewhat less negative ORPs (ca. −500 mV vs Ag/AgCl), presumably because of less contact between deposited particles and the electrode and less deposition due to greater settling of the aggregates from suspension.

Without the effect of nZVI deposited directly onto the electrode, even high concentrations of Fe^{2+} produce ORPs only as low as −400 mV vs Ag/AgCl. Microsized ZVI settles quickly without any deposition to the electrode, so all of the ORP response in this system must be due to Fe^{II} from corrosion of the Fe^0. This is consistent with the distinctly slower decline in measured ORP to an ORP_{min} around −200 mV vs Ag/AgCl (Figure 5). Like nZVI, nano Fe_2O_3 and Fe_3O_4 (likely components of the oxidation products of nZVI[12,13,49]) gave stable suspensions during these experiments and visible deposition of particles onto the electrode. However, unlike nZVI, the contact between these iron oxides and the electrode does not appear to have a significant direct effect on electrode response because the measured ORPs (ca. 0 mV for Fe_3O_4 and 100 mV for Fe_2O_3) are significantly more positive than predicted from thermodynamic calculations (Table S2). The difference between nZVI and these oxides is most likely due to kinetic limitations on dissolution, since the 48 h prequilibration time and solution conditions used in these experiments were unlikely to have produced significant dissolved iron.[42]

Effects of Organic Coatings. In practice, nZVI is usually at least partially coated with organic substances, either by design, to make more stable and mobile suspensions, or due to adsorption of natural organic matter (NOM) from the environment. NOM strongly influences the aggregation[16] and electrochemical properties[42] of nZVI, and a combination of these effects is expected to influence the ORP of nZVI suspensions in the presence of any organic surfactants.

To determine the effect of engineered organic coatings of nZVI, we measured the ORP produced by RNIP-M2, which is similar in composition to RNIP-10DP but coated with polyaspartic acid.[17] The ORP vs time profiles (Figure S1-D) give ORP_{min} values (Figure 4) that are similar between the coated and uncoated RNIP at low nZVI concentration but become less negative for RNIP-M2 at higher nZVI concentrations, resulting in a large (∼200 mV) difference in ORP_{lim}. (Table S1). The less negative ORPs obtained for RNIP-M2 are consistent with insulation of the nZVI from the electrode surface (by coating the particles or the electrode, or both, with organic matter). The convergence between ORP_{min} for RNIP-M2 and RNIP-10DP at low nZVI concentration may arise because they were prepared by dilution of the RNIP-M2 stock solution with carbonate buffer. This dilution is analogous with what happens during injection of RNIP-M2 into the subsurface and therefore represents another factor that complicates the interpretation of ORP for monitoring the in situ effects of nZVI emplacement.

As we have described elsewhere,[42] the effects of NOM on corrosion of particulate iron can be variable and complex, but the main effect of adding NOM to suspensions of RNIP-10DP was to shift the ORP vs time profiles to more positive values (Supporting Information, Figure S8). This is consistent with the effect seen with RNIP-M2 and probably arises from the same mechanism. In the case of NOM, however, a significant effect on ORP is only seen at artificially high concentrations of organic matter; below ∼10 mg/L NOM, the effect on ORP appears to be insignificant.

Implications for Monitoring nZVI under Field Conditions. The results presented here show that even for laboratory model systems that afford considerable control over experimental conditions, the response of ORP electrodes to suspensions of nZVI is not a simple function of nZVI concentration. At high concentrations of nZVI, ORP is dominated by direct interaction between the electrode and the nZVI particles, but this response is nonlinear and saturates with increased coverage of the electrode surface with adsorbed particles. Under these conditions, the presence of nZVI is visually apparent, and ORP measurements add little additional information about the concentration or condition of the particulate material. At low nZVI concentrations, the measured ORP is a mixture of contributions that includes adsorbed nZVI and the dissolved H_2 and Fe^{II} species that arise from corrosion of nZVI. Since all of these redox active species give potentials that fall in the same range, ORP measurements cannot distinguish their concentrations. This lack of specificity is compounded for field applications because of the possibility that nZVI and its corrosion products will be affected differently by transport, resulting in partial separation of these species into zones. Conversely, however, ORP measurements may provide useful information when applied in combinations (e.g., Pt vs GC electrodes) or with complementary characterizations (e.g., concentrations of dissolved iron or hydrogen). ORP measurements made under controlled laboratory conditions—such as with the rotating disk electrodes used here—may prove to be useful in unexpected ways, such as for in situ monitoring of nZVI deposition to surfaces.

■ ASSOCIATED CONTENT

Supporting Information. Method details, additional RDE results, LSV results, thermodynamic calculations, and analysis of the effects of dissolved H_2 and O_2. This material is available free of charge via the Internet at http://pubs.acs.org.

■ AUTHOR INFORMATION

Corresponding Author
*Phone: (503)748-1023. Fax: (503)748-1464. E-mail: tratnyek@ebs.ogi.edu.

■ ACKNOWLEDGMENT

This work was supported primarily by the Strategic Environmental Research and Development Program (SERDP) under Project ER-1485 and secondarily by the U.S. Department of Energy (DOE) Division of Chemical Sciences, Geosciences, and Biosciences through Project ER64222-1027803-0012001. This report has not been subject to review by either agency and therefore does not necessarily reflect their views and no official endorsement should be inferred. Samples of nZVI were donated by Toda Americas Corp.

■ REFERENCES

(1) Tratnyek, P. G.; Johnson, R. L. Nanotechnologies for environmental cleanup. *NanoToday* **2006,** *1*, 44–48.

(2) Lowry, G. V. Nanomaterials for groundwater remediation. *In Environmental Nanotechnology*; Wiesner, M. R., Bottero, J.-Y., Eds.; McGraw Hill: New York, 2007; pp 297−336.

(3) Geiger, C. L.; Carvalho-Knighton, K.; Novaes-Card, S.; Maloney, P.; DeVor, R. A review of environmental applications of nanoscale and microscale reactive metal particles. In *Environmental Applications of Nanoscale and Microscale Reactive Metal Particles*; Geiger Cherie, L., Carvalho-Knighton, K. M., Eds.; American Chemical Society: Washington, DC, 2009; Vol. 1027; pp 1−20.

(4) Nurmi, J. T.; Sarathy, V.; Tratnyek, P. G.; Baer, D. R.; Amonette, J. E.; Linehan, J. C.; Karkamkar, A. Recovery of iron/iron oxide nanoparticles from aqueous media: A comparison of methods and their effects. *J. Nanopart. Res.* **2010**, published online (DOI: 10.1007/s11051-11010-19946-x).

(5) Wang, Q.; Snyder, S.; Kim, J.; Choi, H. Aqueous ethanol modified nanoscale zerovalent iron in bromate reduction: Synthesis, characterization, and reactivity. *Environ. Sci. Technol.* **2009,** *43*, 3292–3299.

(6) Zhan, J.; Sunkara, B.; Le, L.; John, V. T.; He, J.; McPherson, G. L.; Piringer, G.; Lu, Y. Multifunctional colloidal particles for in situ remediation of chlorinated hydrocarbons. *Environ. Sci. Technol.* **2009,** *43*, 8616–8621.

(7) Kim, H.-S.; Ahn, J.-Y.; Hwang, K.-Y.; Kim, I.-K.; Hwang, I. Atmospherically stable nanoscale zero-valent iron particles formed under controlled air contact: Characteristics and reactivity. *Environ. Sci. Technol.* **2010,** *44*, 1760–1766.

(8) Phenrat, T.; Saleh, N.; Sirk, K.; Tilton, R. D.; Lowry, G. V. Aggregation and sedimentation of aqueous nanoscale zerovalent iron dispersions. *Environ. Sci. Technol.* **2007,** *41*, 284–290.

(9) Nurmi, J. T.; Tratnyek, P. G.; Sarathy, V.; Baer, D. R.; Amonette, J. E.; Pecher, K.; Wang, C.; Linehan, J. C.; Matson, D. W.; Penn, R. L.; Driessen, M. D. Characterization and properties of metallic iron nanoparticles: Spectroscopy, electrochemistry, and kinetics. *Environ. Sci. Technol.* **2005,** *39*, 1221–1230.

(10) Martin, J. E.; Herzing, A. A.; Yan, W.; Li, X.-Q.; Koel, B. E.; Kiely, C. J.; Zhang, W.-X. Determination of the oxide layer thickness in core-shell zerovalent iron nanoparticles. *Langmuir* **2008,** *24*, 4329–4334.

(11) Liu, Y.; Phenrat, T.; Lowry, G. V. Effect of TCE concentration and dissolved groundwater solutes on NZVI-promoted TCE dechlorination and H_2 evolution. *Environ. Sci. Technol.* **2007,** *41*, 7881–7887.

(12) Sarathy, V.; Tratnyek, P. G.; Nurmi, J. T.; Baer, D. R.; Amonette, J. E.; Chun, C.; Penn, R. L.; Reardon, E. J. Aging of iron nanoparticles in aqueous solution: effects on structure and reactivity. *J. Phys. Chem. C* **2008,** *112*, 2286–2293.

(13) Reinsch, B. C.; Forsberg, B.; Penn, R. L.; Kim, C. S.; Lowry, G. V. Chemical transformations during aging of zerovalent iron nanoparticles in the presence of common groundwater dissolved constituents. *Environ. Sci. Technol.* **2010,** *44*, 3455–3461.

(14) Hydutsky, B. W.; Mack, E. J.; Beckerman, B. B.; Skluzacek, J. M.; Mallouk, T. E. Optimization of nano- and microiron transport through sand columns using polyelectrolyte mixtures. *Environ. Sci. Technol.* **2007,** *41*, 6418–6424.

(15) Kanel, S. R.; Choi, H. Transport characteristics of surface-modified nanoscale zero-valent iron in porous media. *Water Sci. Technol.* **2007,** *55*, 157–162.

(16) Johnson, R. L.; O'Brien Johnson, R.; Nurmi, J. T.; Tratnyek, P. G. Natural organic matter enhanced mobility of nano zero-valent iron. *Environ. Sci. Technol.* **2009,** *43*, 5455–5460.

(17) Phenrat, T.; Kim, H.-J.; Fagerlund, F.; Illangasekare, T.; Tilton, R. D.; Lowry, G. V. Particle size distribution, concentration, and magnetic attraction affect transport of polymer-modified Fe^0 nanoparticles in sand columns. *Environ. Sci. Technol.* **2009,** *43*, 5079–5085.

(18) Elliott, D. W.; Zhang, W.-X. Field assessment of nanoscale bimetallic particles for groundwater treatment. *Environ. Sci. Technol.* **2001,** *35*, 4922–4926.

(19) Wei, Y.-T.; Wu, S.-C.; Chou, C.-M.; Che, C.-H.; Tsai, S.-M.; Lien, H.-L. Influence of nanoscale zero-valent iron on geochemical properties of groundwater and vinyl chloride degradation: A field case study. *Water Res.* **2010,** *44*, 131–140.

(20) He, F.; Zhao, D.; Paul, C. Field assessment of carboxymethyl cellulose stabilized iron nanoparticles for in situ destruction of chlorinated solvents in source zones. *Water Res.* **2010,** *44*, 2360–2370.

(21) Quinn, J.; Elliott, D.; O'Hara, S.; Billow, A. Use of nanoscale iron and bimetallic particles for environmental remediation: A review of field-scale applications. In *Environmental Applications of Nanoscale and Microscale Reactive Metal Particles*; Geiger Cherie, L., Carvalho-Knighton, K. M., Eds.; American Chemical Society: Washington, DC, 2009; Vol. 1027; pp 263−283.

(22) Simonet, B. M.; Valcárcel, M. Monitoring nanoparticles in the environment. *Anal. Bioanal. Chem.* **2009,** *393*, 17–21.

(23) Tratnyek, P. G.; Scherer, M. M.; Johnson, T. J.; Matheson, L. J. Permeable reactive barriers of iron and other zero-valent metals. In *Chemical Degradation Methods for Wastes and Pollutants: Environmental and Industrial Applications*; Tarr, M. A., Ed.; Marcel Dekker: New York, 2003; pp 371−421.

(24) Morris, J. C.; Stumm, W. Redox equilibria and measurements of potentials in the aquatic environment. In *Equilibrium Concepts in Natural Water Systems*; American Chemical Society: Washington, DC, 1967; pp 270−285.

(25) Whitfield, M. Thermodynamic limitations on the use of the platinum electrode in Eh measurements. *Limnol. Oceanogr.* **1974,** *19*, 857–865.

(26) Hostettler, J. D. Electrode electrons, aqueous electrons, and redox potentials in natural waters. *Am. J. Sci.* **1984,** *284*, 734–759.

(27) Peiffer, S.; Klemm, O.; Pecher, K.; Hollerung, R. Redox measurements in aqueous solutions—A theoretical approach to data interpretation based on electrode kinetics. *J. Contam. Hydrol.* **1992,** *10*, 1–18.

(28) Grundl, T. Determination of redox status in sediments. In *Metal Contaminanted Aquatic Sediments*; Ann Arbor: Ann Arbor, MI, 1995; pp 149−167.

(29) Spiro, M. Polyelectrodes: The behaviour and applications of mixed redox systems. *Chem. Soc. Rev.* **1986,** *15*, 141–165.

(30) Oman, S. F. On the seventieth anniversary of the "Suspension Effect": A review of its investigations and interpretations. *Acta Chim. Slov.* **2000,** *47*, 519–534.

(31) Oman, S. F.; Camoes, M. F.; Powell, K. J.; Rajagopalan, R.; Spitzer, P. Guidelines for potentiometric measurements in suspensions. Part A. The suspension effect: (IUPAC technical report). *Pure Appl. Chem.* **2007,** *79*, 67–79.

(32) Oman, S. F.; Camoes, M. F.; Powell, K. J.; Rajagopalan, R.; Spitzer, P. Guidelines for potentiometric measurements in suspensions. Part B. Guidelines for practical pH measurements in soil suspension (IUPAC Recommendations 2006). *Pure Appl. Chem.* **2007,** *79*, 81–86.

(33) Oman, S. F. Electrode potentials in suspensions interpreted as a mixed potential. *Acta Chim. Slov.* **2004,** *51*, 189–201.

(34) Grundl, T. Redox inactivity of colloidal ferric oxyhydroxide solids. *J. Contam. Hydrol.* **1992,** *9*, 369–377.

(35) Grenthe, I.; Stumm, W.; Laaksuharju, M.; Nilsson, A. C.; Wikberg, P. Redox potentials and redox reactions in deep groundwater systems. *Chem. Geol.* **1992,** *98*, 131–150.

(36) Henglein, A. Physicochemical properties of small metal particles in solution: "microelectrode" reactions, chemisorption, composite metal particles, and the atom-to-metal transition. *J. Phys. Chem.* **1993,** *97*, 5457–5471.

(37) Murray, R. W. Nanoelectrochemistry: Metal nanoparticles, nanoelectrodes, and nanopores. *Chem. Rev.* **2008,** *108*, 2688–2720.

(38) Plieth, W. J. Electrochemical properties of small clusters of metal atoms and their role in the surface enhanced Raman scattering. *J. Phys. Chem.* **1982,** *86*, 3166–3170.

(39) Liver, N.; Nitzan, A. Redox properties of small semiconductor particles. *J. Phys. Chem.* **1992,** *96*, 3366–3373.

(40) Scherer, M. M.; Balko, B. A.; Tratnyek, P. G. The role of oxides in reduction reactions at the metal-water interface. In *Mineral-Water Interfacial Reactions: Kinetics and Mechanisms*; Sparks, D. L., Grundl, T. J., Eds.; American Chemical Society: Washington, DC, 1998; *ACS Symp. Ser.* 715; pp 301−322.

(41) Nurmi, J. T.; Bandstra, J. Z.; Tratnyek, P. G. Packed powder electrodes for characterizing the reactivity of granular iron in borate solutions. *J. Electrochem. Soc.* **2004,** *151*, B347–B353.

(42) Nurmi, J. T.; Tratnyek, P. G. Electrochemical studies of packed iron powder electrodes: Effects of common constituents of natural waters on corrosion potential. *Corros. Sci.* **2008,** *50*, 144–154.

(43) Kita, H. Periodic variation of exchange current density of hydrogen electrode reaction with atomic number and reaction mechanism. *J. Electrochem. Soc.* **1966,** *113*, 1095–1106, 1107–1010.

(44) Harinipriya, S.; Sangaranarayanan, M. V. Hydrogen evolution reaction on electrodes: Influence of work function, dipolar adsorption, and desolvation energies. *J. Phys. Chem. B* **2002,** *106*, 8681–8688.

(45) Yao, K.-M.; Habibian, M. T.; O'Melia, C. R. Water and waste water filtration. Concepts and applications. *Environ. Sci. Technol.* **1971,** *5*, 1105–1112.

(46) Hansson, E. B.; Odziemkowski, M. S.; Gillham, R. W. Formation of poorly crystalline iron monosulfides: Surface redox reactions on high purity iron, spectroelectrochemical studies. *Corros. Sci.* **2006,** *48*, 3767–3783.

(47) Sawyer, D. T.; Sobkowiak, A.; Roberts, J. L. J. *Electrochemistry for Chemists*; Wiley: New York, 1995.

(48) Macalady, D. L.; Langmuir, D.; Grundl, T.; Elzerman, A. Use of model-generated Fe^{3+} ion activities to compute Eh and ferric oxyhydroxide solubilities in anaerobic systems. In *Chemical Modeling of Aqueous Systems II*; American Chemical Society: Washington, DC, 1990; Vol. 416; pp 350−367.

(49) Reinsch, B. C.; Lowry, G. V.; Kim, C. S. EXAFS analysis of reactive nanoscale iron oxidation in water. *Geochim. Cosmochim. Acta* **2007,** *71*, A830–A830.